DYNAMIC ANALYSIS OF DOLPHIN-STYLE THERMAL CROSS-COUNTRY FLIGHT

Dr. József Gedeon
Technical University
Budapest, Hungary

Presented at the 14th OSTIV Congress, Waikerie, Australia (1974)

Continuation paper (Part I) presented at the 13th OSTIV Congress
and published in OSTIV Publication XII

Continuing the work reported on in Part I, a second thermal model patterned after Konovalov type "a" thermals has been introduced. Circling cross-country flight calculations and quasi-static dolphin flight calculations using "square shaped" thermals have been made in order to get a basis for comparison. The computer program doing the two degrees of freedom dynamic calculations has also been improved upon.

Analysis of a fair number of computer runs using both the first and the second thermal model seems to recommend following flight tactics:

a. A medium level of load factors and climb/dive angles looks to be the best choice ($n_L \cong 1.8$, $n_G \cong 0.56$, $\Theta_H \cong 21^o$).

b. As for the optimum place to initiate the pull-up, there are two alternatives. In order to get maximum energy gain from the thermal, i.e. when aiming for optimum glide distance, the pull-up has to be started some $3R_\infty$ to $5R_\infty$ before entering the up-draft. The correct pull-up point for best cross-country speed is in the thermal core, in case of the second thermal model at some $1.0\ R_\infty$ to $1.5\ R_\infty$ after entering the updraft. Taking into account the lag due to pilot reaction time and the lag time constant of the sailplane longitudinal short period motion a pull-up decision at the point of entering the core may be recommended.

INTRODUCTION

In Part I of the paper, presented at the 13th Congress (1), the author attempted to develop a computer procedure for taking into account some important dynamic losses in the flight path calculations of dolphin-style traverses through thermals. Incentives to start this work were the seemingly general lack of sound theory/simple instrumentation combination, to quote the well known MacCready theory and ring or special instrument for circling thermal cross-country work by way of example, to enable this type of flying to be done most effectively and the fact that previous papers known to the author (2, 3) do not go beyond quasi-static treatment of the problem.

Since then several papers on the subject have been published - e.g. that of ANTWEILER (4) giving an ingenious graphical method of computing the cross-country speed - but all those known to the author deal with the problem by way of quasi-static methods, the most effective technique of piloting the transient sections of the flight (taking into account the limiting conditions and additional losses imposed by finite maneurverability of the glider) remaining unsolved. A continuation of the work, therefore, appeared to be worthwhile and the results are given in this Part II of the paper.

NOTATION

c	thermal lift	m sec^{-1}
c_o	maximal thermal lift	m sec^{-1}
g	gravity acceleration	m sec^{-2}
n	normal load factor	
v	sailplane speed (in wind co-ordinates)	m sec^{-1}
v_H	correct speed to initiate push-over or pull-up	m sec^{-1}
w	rate of climb	m sec^{-1}
w_{min}	sailplane minimal sink (from speed polar curve)	m sec^{-1}
x	distance from centre of thermal	m
H	height gain	m
$H_D = H + (v^2-v_s^2)/2g$	energy height gain	m
R	(nominal) thermal radius	m
R_∞	theoretical minimal radius of turn	m
L	updraft section length	m
S	spacing of thermals	m
S_G	length of re-accelerating	m
S_L	length of slowing-down	m
V	sailplane speed (in wind co-ordinates)	km h^{-1}
V_{AT}	cross-country speed for zero wind	km h^{-1}
$\beta=(0.5L-X_A)/R_\infty$	pull-up lead coefficient	
γ	energy gain coefficient	
ϵ	glide ratio	
η_s	glide coefficient	
η_v	speed coefficient	
$\varphi = c_o R/w_{min} R_\infty$	thermal number	
θ	glide angle (in wind co-ordinates)	o
θ_H	climb angle for middle part of slow-down section (in wind co-ordinates)	o

Subscripts

e	climb	D	at point D
s	glide	G	push-over
A	at point A	L	pull-up
B	at point B	2.5R	at point x = 2.5R
C	at point C	5R	at point x = 5R

Superscripts — quasi-static idealized conditions, "square thermal"

1. Thermal Models

Dynamic dolphin-flight calculations reported in Part I were based on the isolated thermal model having the updraft profile

$$c = c_o e^{-\left(\frac{x}{R}\right)^2}\left[1-\left(\frac{x}{R}\right)^2\right] \qquad (1)$$

with maximum updraft c_o and nominal thermal radius R as free parameters (Fig. 1). The thermal field was supposed to consist of identical thermals of equal spacing S. In order to give some basis for pre-estimating the accuracy to be expected while using this model, isolated thermal profiles as given by WOODWARD (5) Fig. 2, and as given by KONOVALOV (6) Fig. 1, type "b", are reproduced in Fig. 2. It may be seen that there is a substantial difference between the two experimental results, the profile given by Equ. (1) and Fig. 1 lying between them and fairly close to the values reported by Konovalov.

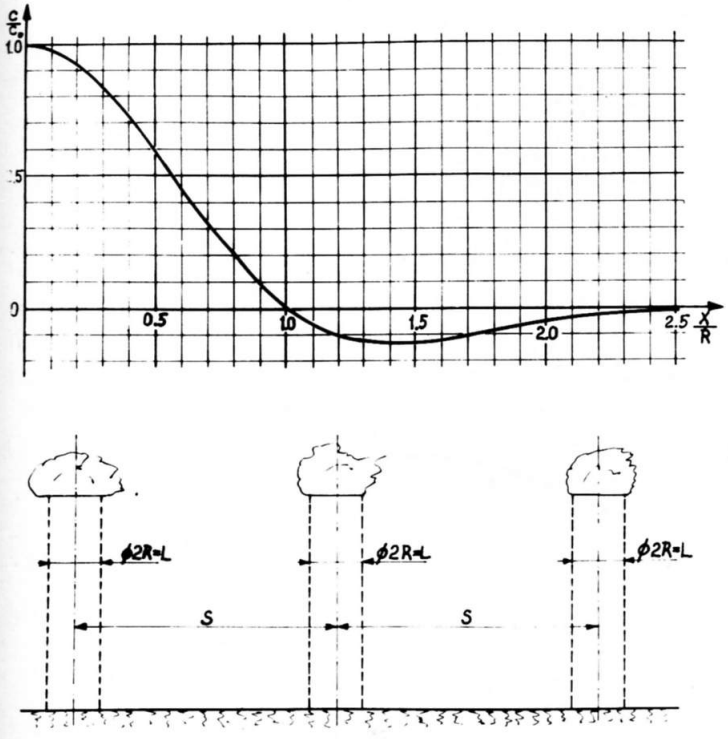

FIGURE 1. Isolated Thermal and Thermal Street Model.

Sustained dolphin flight using only isolated thermals is rarely, if ever, made, so a need was felt to fill the gap between the isolated thermal and the fully developed cloud street. Fortunately, KONOVALOV has reported on multi-cell thermal structures also (6) Fig. 1, type "a", an early confirmation of his results for a country of different climate is given by MILFORD (7). Stimulated by these, an attempt was made to extend Equ. (1) to cover a four-cell, blended-core thermal structure. After some trials, the following formula was arrived at:

$$c = c_o\left\{\frac{13}{11}e^{-\left(\frac{x+2R}{R}\right)^2}\left[1-\left(\frac{x+2R}{R}\right)^2\right]+\right.$$

$$\frac{4}{3}e^{-\left(\frac{x+\frac{2}{3}R}{R}\right)^2}\left[1-\left(\frac{x+\frac{2}{3}R}{R}\right)^2\right]+$$

$$\frac{4}{3}e^{-\left(\frac{x-\frac{2}{3}R}{R}\right)^2}\left[1-\left(\frac{x-\frac{2}{3}R}{R}\right)^2\right]+\frac{13}{11}e^{-\left(\frac{x-2R}{R}\right)^2}$$

$$\left.\left[1-\left(\frac{x-2R}{R}\right)^2\right]\right\} \qquad (2)$$

The profile given by Equ. (2) may be seen and compared to the Konovalov profile type "a" in Fig. 3. In the outer parts of the lift area there is a systematic error but in view of the limited number of test results known to the author the theoretically attractive principle of equal inner core spacing appears to be justified. The lift area as given by Equ. (2) extends from $x = -89/30\ R$ to $x = +89/30\ R$ the updraft section length being $L = 89/15\ R = 5.9\overline{3}\ R$. For practical purposes the border of influence of the thermal group, i.e. the downdraft region boundary, may be set at $x = \pm 5R$. This thermal model may be referred to as type 2, or four-cell or group model as opposed to the type 1, or single-cell or isolated thermal profile given by Equ. (1).

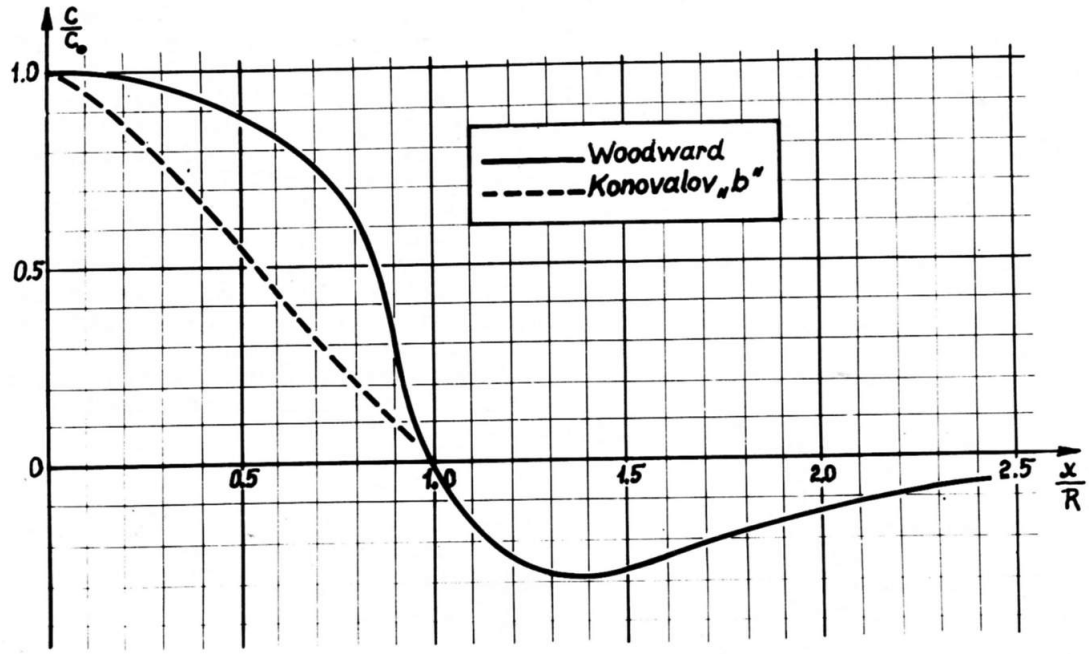

FIGURE 2. Thermal Profiles as Given by Woodward (Ref. 5) and by Konovalov (Ref. 6, type "b").

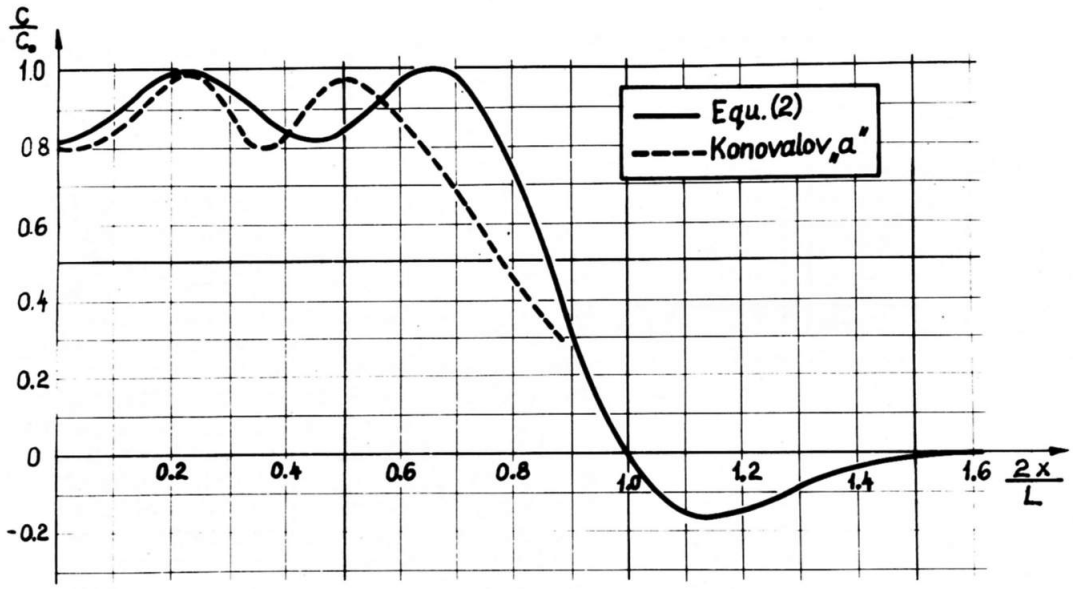

FIGURE 3. Four-Cell Thermal Profiles Konovalov Type "a" (Ref. 6) as given by Equation (2).

Looking for optima in multi-parameter problems by way of numerical methods can be intricate and laborious so a comparative quasi-static, idealized cross-country speed calculation may not be out of place. For that purpose a thermal field composed of "square" thermals of uniform constant $c=c_o$ lift along the traverse length L and with uniform downdraft $-0.07c_o$ between the thermals was adopted.

2. Computer Program Improvements

As already described in Part I, the computer program was built around three types of path elements:

- procedure SIKL (for GLIDE) giving constant speed flight;
- procedure DELF (for DOLPHIN) to compute flight path sections with prescribed constant normal acceleration;
- procedure KIFUT (for RUN DOWN) giving constant attitude flight, conceived originally to smooth out minor speed differences between adjacent sections but employed later in more general roles also.

Correct sequencing of these path elements to give the desired flight profile seemed to be a straightforward matter at first but in practice this turned out not to be the case. A considerable amount of computer time had to be spent in "teaching the program to fly". Difficulties centered around arriving at a smooth transition between the end of the slow-down and re-accelerate sections and the beginning of the following climb glide sections respectively. The present state-of-the-art in program organization is to be seen at the flowchart on Fig. 4.

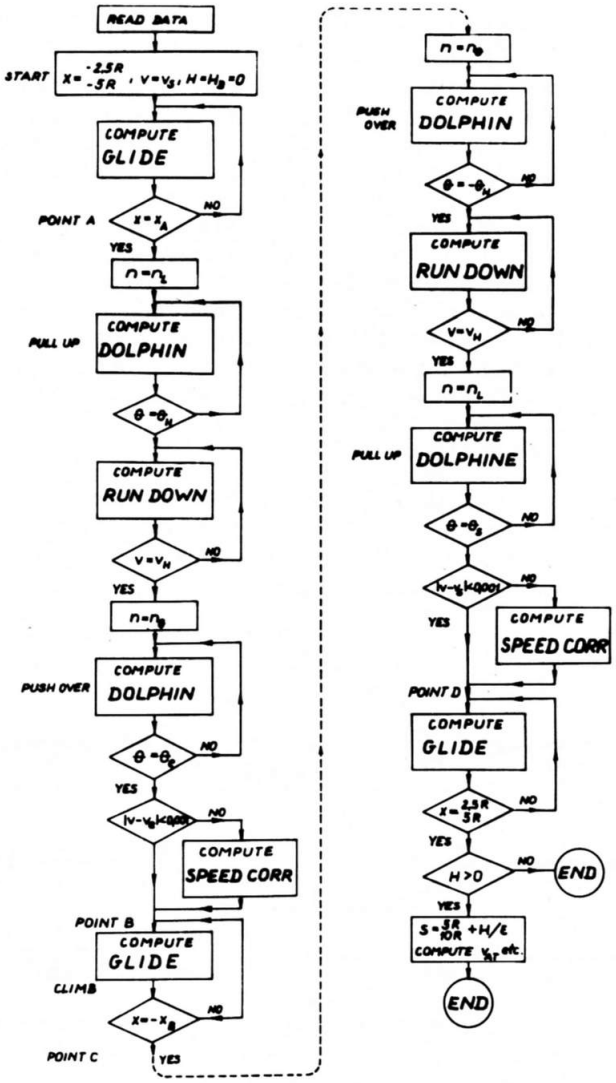

FIGURE 4. Flowchart of the Revised Computer Program.

The starting point is at $x = -2.5R$ for single-cell thermal traverses and at $x = -5R$ for four-cell ones. Constant speed glide is computed to point $x = x_A$. At this point, before entering the pull-up phase of the slow-down section, with the knowledge of v_e and θ_H a crude value of the speed to initiate push-over (v_H) is worked out. Pull-up is made with prescribed constant normal acceleration n_L until θ_H. From this point constant attitude flight using procedure RUN DOWN is followed until speed is reduced to v_H. (In describing the program all speed values are given in lower-case letters, because the program is using m sec units, conversion of the cross-country speed to km h units being done only before print out.) After the following push-over with n_G minor differences to the desired gliding speed in the

central climbing section of the traverse (v_e) may still occur. Therefore, after the level-out, a control for speed difference is made and one or two speed correction sections are inserted if necessary. Speed correction sections are composed of twin short arcs of push over and pull up (in that order for speed gain and in the reverse for slowing down) using procedure DOLPHIN. A similar cycle of events takes place at the re-accelerate section end in correct sequence. Computing the glide distance S and the cross-country speed V_{AT} are done as previously.

Using this method consistent smooth transitions are achieved. Progress in this domain may be judged by comparing Fig. 5 and 6 to Fig. 5 of Part I.

3. Circling Cross-Country Speed

Circling thermal cross-country flight calculations and tactics are theoretically well-founded and proven by many years of practical experience. It was, therefore, thought advisable to make a short review of circling performance data calculated using the same ASW 15 polar against corresponding results of dolphin flight calculations. To facilitate the comparison, circling flight data will be presented in a somewhat unusual form.

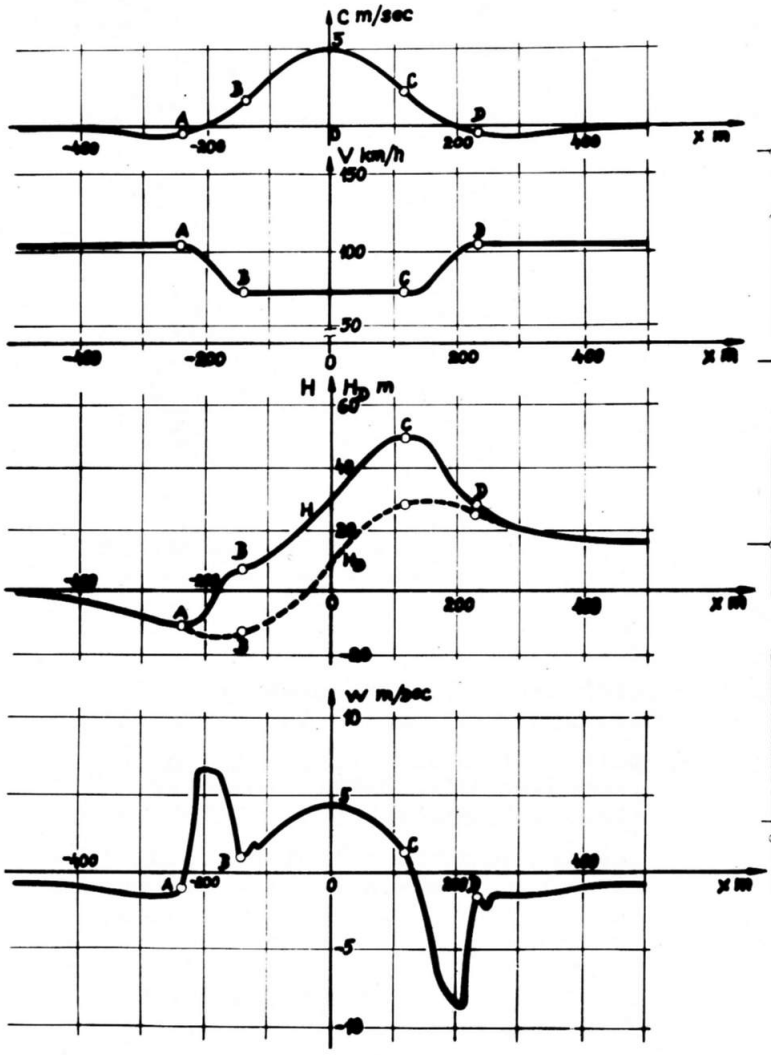

FIGURE 5. Traverse of a 5 m/sec Single-Cell Thermal Type 1.

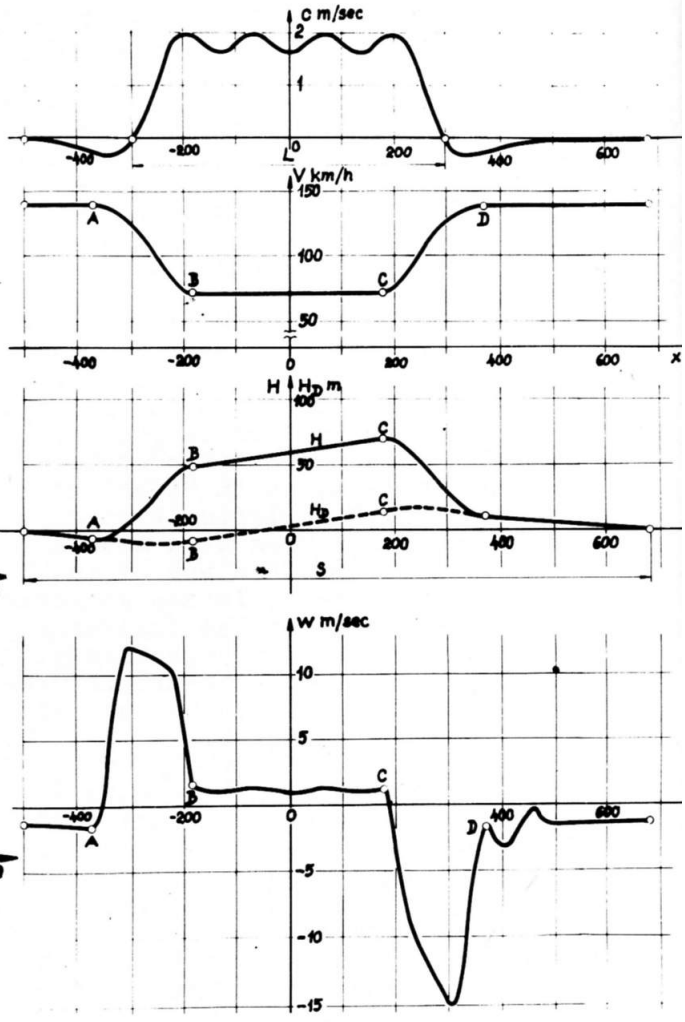

FIGURE 6. Traverse of a 2 m/sec Four-Cell Thermal Type 2.

If we are intending to begin our calculations in a completely idealized form, we can start from a very large-sized "square" thermal in which the glider could do its circles practically without banking with a relative sink w_{min}. In this case, for a given thermal strength, cross-country speeds would depend only on the glide speed between thermals (V_s) and hence on the glide ratio $H/S = \epsilon_s$ as shown on Fig. 7. Optima of the curves correspond to the well-known MacCready speeds. Optimum rates of climb in circling are considerably below those underlying the results given in Fig. 7 due to increased relative sink in banked circling flight. Rate of climb ratios as function of the thermal number φ for a number of type 1 isolated thermals of different strength and nominal radius are to be seen on Fig. 8. There is no possibility for climbing below φ = 9 to 10°, for good climb ratios a value of $\varphi \geq 40^{\circ}$ being necessary.

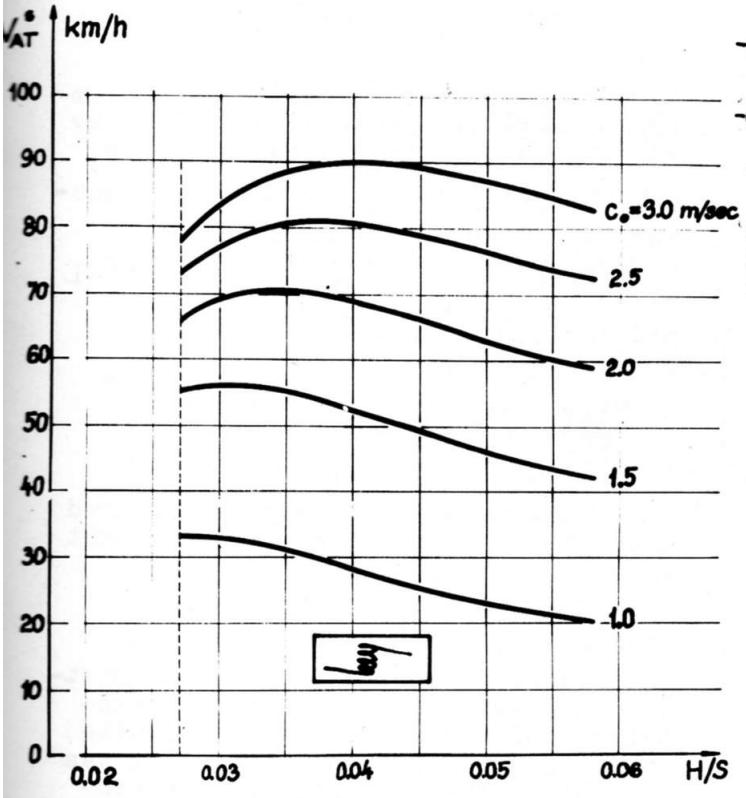

FIGURE 7. Cross-Country Speeds in Idealized Circling Flight.

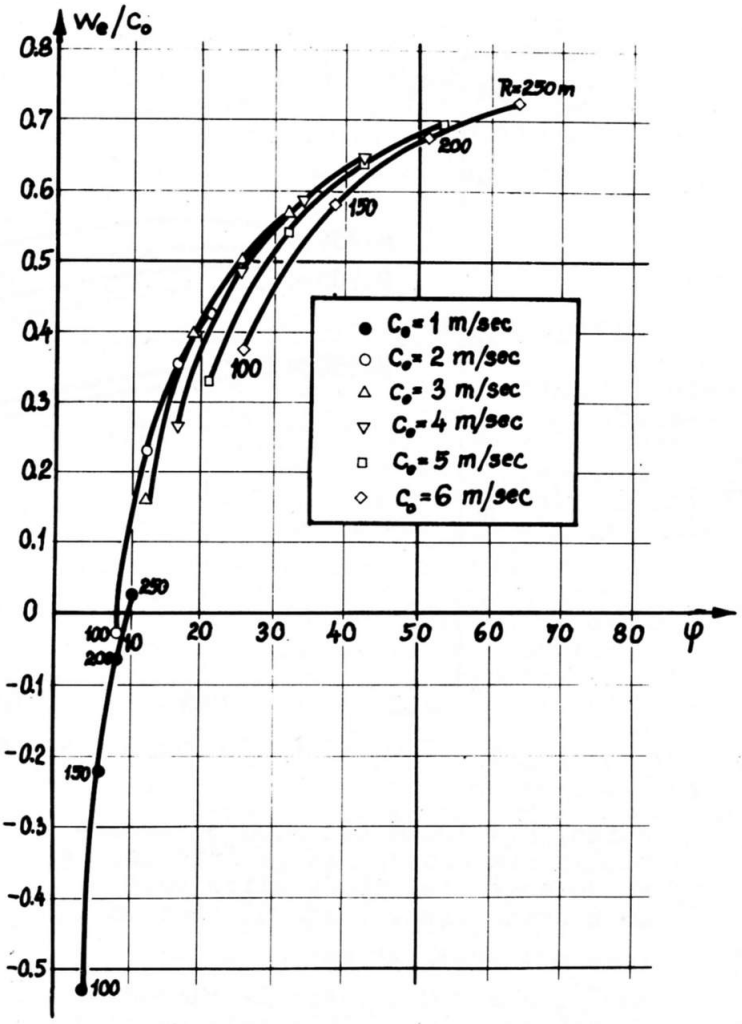

FIGURE 8. Rate of Climb in Type 1 Thermals.

The reduction in rate of climb due to banking and to the decrease of lift in the outer parts of the thermal is well suited to theoretical/numerical treatment. There is much more uncertainty in accounting for another practical difficulty in optimal utilization of the thermal lift: the time spent in reduced climb while searching for the center of the thermal. This problem has been circumvented by assuming only $w_e/2$ for the first 30 seconds of the climb.

Cross-country speeds calculated this way for type 1 c_o = 2 m sec^{-1} thermals are given in Fig. 9. To avoid confusion, only the curves for the lowest and greatest height of

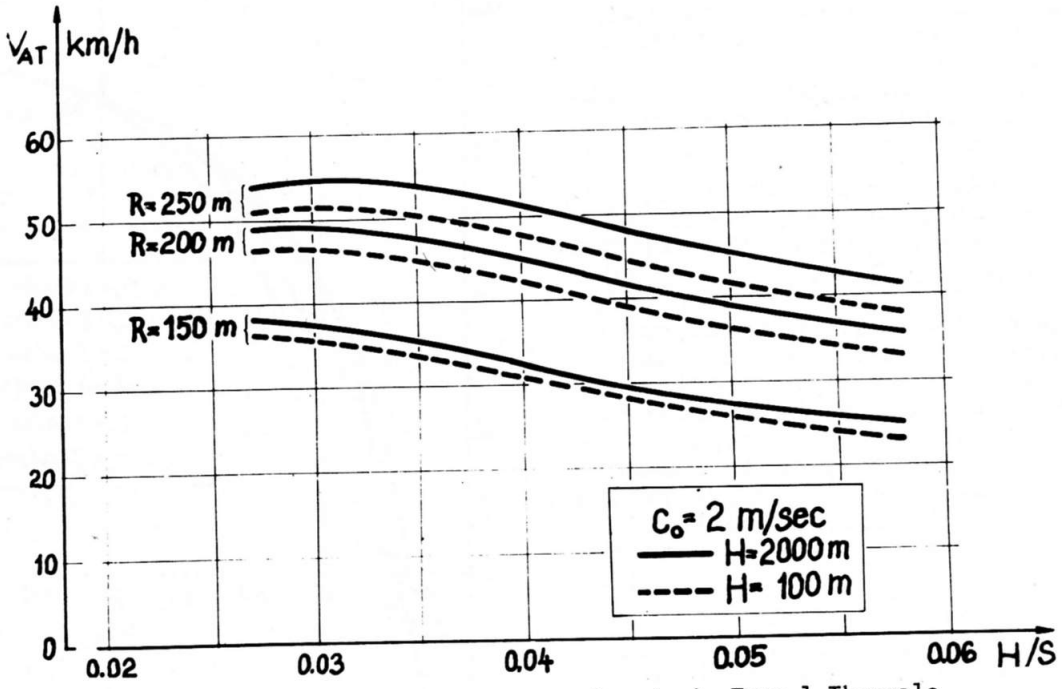

FIGURE 9. Circling Cross-Country Speeds in Type 1 Thermals.

climb, H = 100 m and 2000 m respectively are shown. It is interesting to do some elementary slide rule work using Figs. 7 and 9. Let us take a thermal street of c_o = 2 m sec^{-1}, R = 200 m thermals placed S = 25 km apart. In idealized conditions a best cross-country speed V^*_{AT} = 70.5 km h^{-1} would be obtainable at H/S = 0.034 by doing H = 850 m climbs in the thermals and gliding with the speed appropriate for this gliding ratio between them. Entering with the same values in Fig. 9 shows a cross-country speed of about V_{AT} = 46 km h^{-1} the ratio of real to idealized cross-country speeds being this time:

$$\frac{V_{AT}}{V^*_{AT}} = \frac{46}{70.5} = 0.652$$

Fig. 9 shows a possibility to improve slightly upon this situation by gliding between the thermals with V_s corresponding th ϵ_s = 0.029 and reducing the height of climb to H = 0.029x25000 = 725 m. Cross-Country speed will mount to V_{AT} = 47.5 km h^{-1} and the speed ratio will be:

$$\frac{V_{AT}}{V^*_{AT}} = \frac{47.5}{70.5} = 0.674$$

Results as these may be compared later to corresponding dolphin flight values.

4. Idealized Dolphin Flight

There is no problem in interpreting quasi-stationary, idealized sustained dolphin flight speed formulae for a "square" thermal street; it was thought, therefore, not to be necessary to repeat them here. Those interested could refer e.g. to the paper of TOMCZYK (3)*. On the other hand, for greater values of L/S

---

* When comparing results given by Tomczyk in (3) with those of the present paper, care should be taken not to overlook a difference in notation. Tomczyk is using the same sign L for the updraft section length but S is for the downdraft section length and not for the thermal spacing as here. Our S reads S+L in paper (3).

results of the classical cloud-street flying theory (see e.g. the paper of FAVARGER (8)) may be considered. Cross-country speed depends on thermal strength $c = c_o$, on updraft mileage to total mileage ratio L/S, on the speed in climb V_e and on the glide speed between thermals V_s. For the sake of clarity, no single parameter trends but only best cross-country speeds for a given thermal strength and L/S ratio are represented on Fig. 10. In searching for optima by way of dynamic calculations, results may be set against these idealized values in order to get better insight into the influence of different parameters.

When making comparisons between circling and dolphin flight calculations, H/S values may be converted into corresponding L/S values by knowing - and only by knowing - the value of L. E.g. the numerical example cited in commenting on Fig. 9 should mean a ratio of L/S = 2R/S = 400/25000 = 0.016, a value obviously out of question even for idealized sustained dolphin cross-country flying.

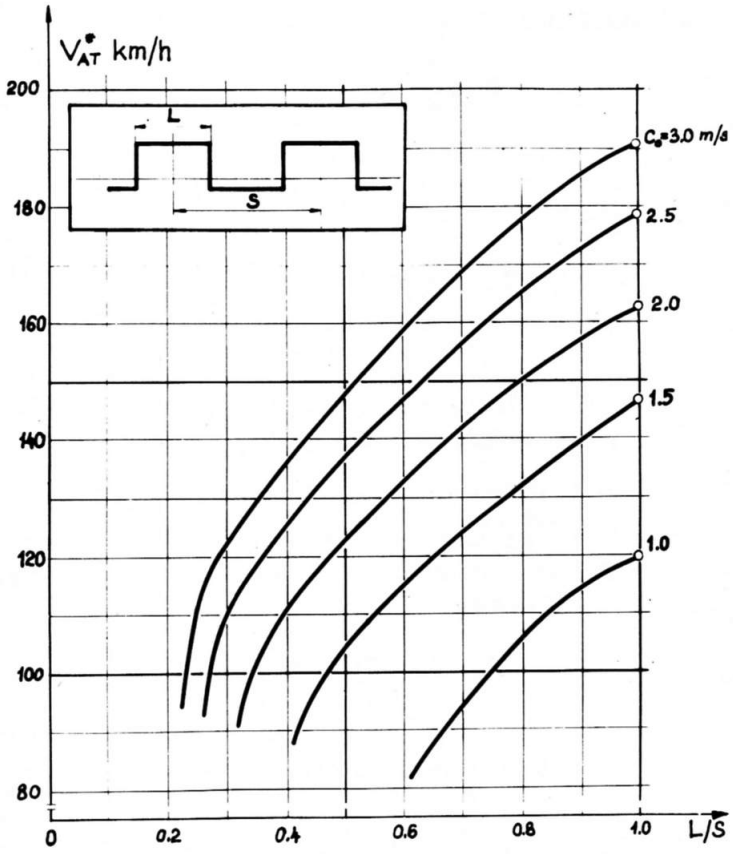

FIGURE 10. Cross-Country Speeds in Idealized Dolphin Flight.

5. Energy Gain and Flight Efficiency

When, after doing a dynamic dolphin-style thermal traverse calculation, a single parameter is altered and then the calculation repeated, both main results of the calculation (cross-country speed and gliding distance to the next thermal) will change. Sad to say, there is no possibility of doing a sequence of one-parameter calculations, say for a fixed value of L/S, in order to get direct optima for speed. This state of affairs necessitated the introduction of efficiency parameters by means of which improvements could be more directly assessed. The three parameters to be proposed in the following will be somewhat arbitrary by the very nature of the problem but they nevertheless fulfil their intended purposes satisfactorily.

Our first look at the development of flight tactics will be for maximum energy gain in crossing the thermal. An obvious measure for this would be the height gain H (or H_D in case of appreciable difference at that point) after crossing the thermal at x = 2.5 R and x = 5 R, respectively. Since calculations will have to be done for different glide speeds between thermals V_s and possibly for different thermal diameters too, use of the following formulae for a gross energy gain coefficient may be recommended (see also Fig. 11):

$$\gamma = (H_{2.5R} + 5R\epsilon_s)/5R \qquad (3a)$$

$$\gamma = (H_{5R} + 10\,R\epsilon_s)/10\,R \qquad (3b)$$

(3a) being for type 1 and (3b) for type 2 thermals, respectively.

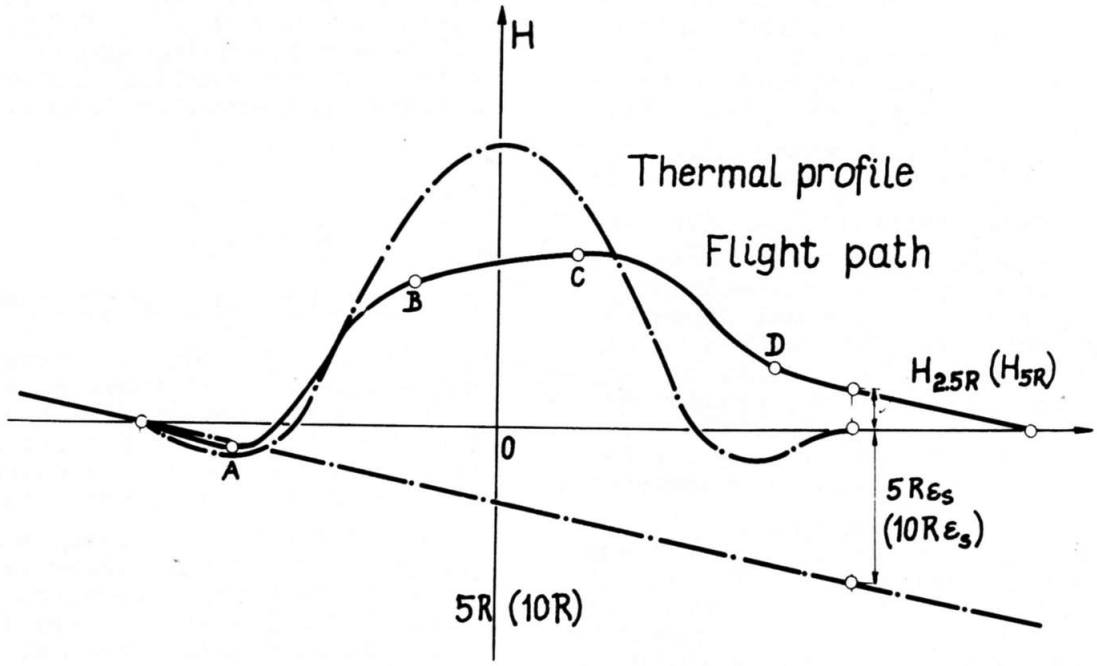

FIGURE 11. Definition of the Energy Gain Coefficient.

Our next concern will be to achieve the greatest possible glide distance to the next thermal and/or the greatest cross-country speed. On this behalf, let us draw the idealized cross-country speed curve of Fig. 10 (e.g. that belonging to thermal strength c_o = 2 m sec^{-1}) not against L/S but against the reciprocal value S/L as shown on Fig. 12. Should the point P, corresponding to the glide distance S/L and to the cross-country speed V_{AT} obtained in a dynamic calculation, be plotted on this graph, the results will be seen to lag below the idealized values both in glide distance and in cross-country speed due to dynamic losses. By projecting P for constant speed, we get to point A giving the idealized glide distance for the same speed S^*/L (point A_1). Doing the same for constant glide distance point B on the idealized curve giving V^*_{AT} (point B_1) may be obtained. It is obvious that we have herewith a possibility of defining a glide coefficient as

$$\eta_S = \frac{S/L}{S^*/L} \tag{4}$$

and a speed coefficient as

$$\eta_V = \frac{V_{AT}}{V^*_{AT}} \tag{5}$$

For the example given on Fig. 12 S/L = 1.94 and V_{AT} = 107.3 km h^{-1} had been computed projections on the idealized curve giving S^*/L = 2.65 and V^*_{AT} = 124.4 km h^{-1} respectively. The value of the glide coefficient is, therefore,

$$\eta_S = \frac{1.94}{2.65} = 0.731$$

and the speed coefficient is

$$\eta_V = \frac{107.3}{124.4} = 0.863$$

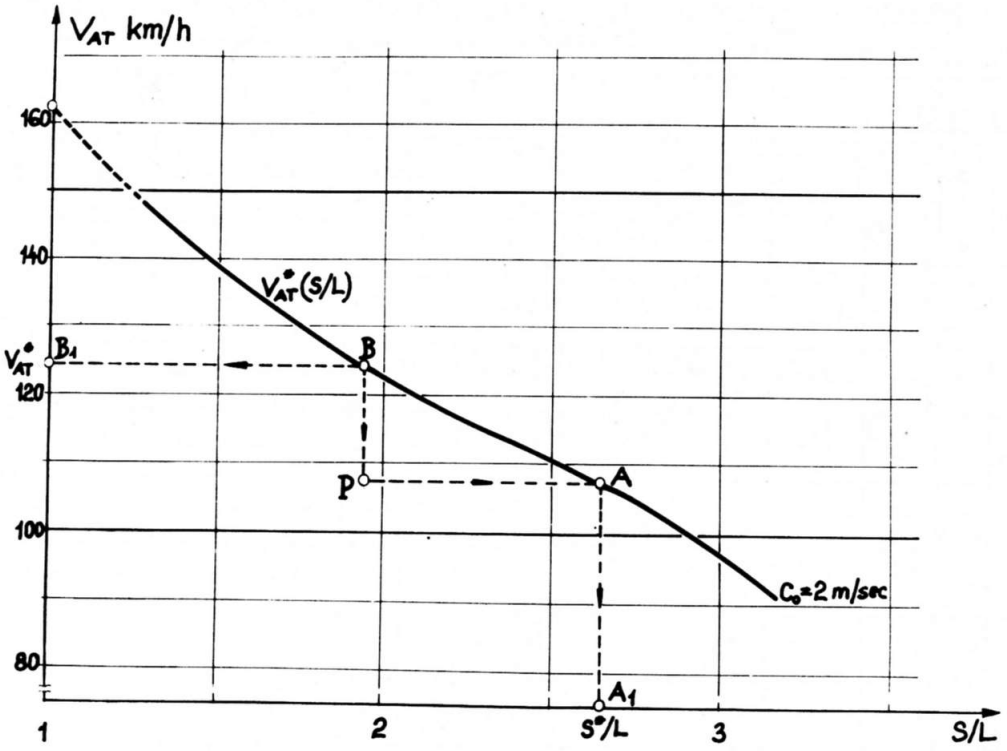

FIGURE 12. Definition of the Glide Coefficient and of the Speed Coefficient.

6. Single-Cell Thermal Crossings

Calculations have been done first on type 1 single-cell thermals as opposed to thermal streets. Parameters and results obtained are given in Table 1 for the 11 runs computed. Values of the energy gain coefficient γ are plotted - using symbols given in Fig. 13 - over the pull-up lead coefficient β on Fig. 14 for all runs. When comparing the results, the following comments may be made:

- no definite maxima for load factors and for climb angle can be claimed from these few runs but moderate values seem to be a fair compromise;
- there is a clear advantage in energy gain for early pull-up;
- the relative density of strong single-cell thermals indicated to be necessary for sustained flight seems to be disproportinately high when compared with meteorological observations.

It was this latter fact which strongly suggested the development of the type 2 four-cell thermal model for which all subsequent calculations have been made.

7. Four-Cell Thermal Crossings

Due to limitations of computer time and man-power, standard values of c_o = 2 m sec^{-1} and R = 100 m were adopted for all type 2 thermal calculations. Parameters and results of the 54 runs done so far are compiled in Table 2. In order to find out some trends, let us take a closer look at a few systematic sequences. For marking of the parameters n_L, m_G and Θ_H in subsequent figures the symbols as given Fig. 15 are used.

Losses in cross-country performance as compared to idealized conditions are primarily attributable to the distance covered while slowing-down and re-accelerating and to the drag increments due to increased

TABLE 1. RESULTS OF SINGLE-CELL THERMAL TRAVERSE COMPUTATIONS

	Thermal c_o			Flight Data						Results							
Run	M sec^{-1}	R m	φ	V_s km h^{-1}	V_e km h^{-1}	n_L	n_G	Θ_H^o	β	S_L/R	S_G/R	S_L/R_∞	S_G/R_∞	$\gamma\ 10^{-2}$	S/L	V_{AT} km h^{-1}	Remarks
1	3.0	200	25.757	139.880	100.38	1.50	0.80	15	1.77	1.150	2.038	6.160	10.92	1.891			S < 5R
2	3.0	200	25.757	139.880	104.58	1.80	0.75	15	2.95	1.143	2.078	6.140	11.14	1.887			S < 5R
3	3.0	200	25.757	139.880	101.09	1.80	0.75	15	4.29	1.134	2.011	6.085	10.78	2.224			S < 5R
4	3.0	300	38.636	139.880	80.65	1.80	0.75	18	4.02	1.298	2.780	10.42	22.35	3.189			S < 5R
5	6.0	200	51.515	139.880	72.092	1.80	0.70	22	2.68	0.937	1.156	5.025	6.195	5.631	3.947	112.343	
6	6.0	200	51.515	139.880	72.092	1.80	0.70	22	2.68	0.936	1.102	5.018	5.915	5.593	4.125	113.545	
7	6.0	200	51.515	103.296	72.092	1.80	0.70	15	0	0.484	0.607	2.595	3.253	5.051	4.710	96.557	
8	6.0	200	51.515	103.296	72.092	1.80	0.70	15	1.072	0.493	0.595	2.641	3.186	5.217	4.840	95.302	
9	6.0	200	51.515	103.296	72.092	1.80	0.70	15	2.357	0.513	0.583	2.747	3.122	5.343	4.939	93.561	
10	5.0	200	42.929	103.296	72.092	1.80	0.70	15	0	0.596	0.749	3.191	4.015	4.160	3.852	95.501	
11	5.0	200	42.929	103.296	72.092	1.80	0.70	15	1.0	0.593	0.719	3.174	3.853	4.317	3.989	94.043	

load factors in pull-ups. It would, therefore, presumably pay to make the distances $S_L = x_B - x_A$ and $S_G = x_D - x_C$ as short as possible using, of course, reasonable load factors. In order to get specific values, transition distances may be compared either to the half of the updraft section length L/2 or to the theoretical minimal radius of turn of the sailplane R_∞. In the former case some measure of the proportions of the thermal utilized imperfectly is shown while the latter can be used in comparing results obtained on different types.

Specific values of transition distance are plotted against glide speed between thermals V_s on Figs. 16-17. For every glide speed, the lowest values are invariably those for the combination $n_L = 1.8$, $n_G = 0.56$ and $\Theta_H = 21^o$. This is, of course, not an absolute statement but transition distances being interesting only in their after-effects, this will be enough to start with.

In the search for optimal conditions, let us pay attention first to energy gain coefficients. It has been concluded from previous investigations that best choices would be medium values of load factors (e.g. around 1.8/0.56) but the role of the climb angle Θ_H has not yet been as clear. On Fig. 18 γ is plotted against Θ_H using identical load factors and for different lead coefficients β. Values obtained this way seem to indicate a mild optimum somewhere around $\Theta_H = 21^o$. For increasing climb angles the straight portions of the transition sections become steadily shorter so there is no point in extending the search to still higher values of Θ_H.

Thermal type: 

N_L	N_S	ϑ_H 15°	18°	22°
1.50	0.80	◆		
1.80	0.75	◇	□	
1.80	0.70	◈		▼

FIGURE 13. Symbols Used on Type 1 Thermal Crossing Charts

Thermal type: 

N_L	N_S	ϑ_H 15°	18°	21°	25°
1.50	0.70		■		
1.80	0.70	⊠	⊞		
1.80	0.56	◇		○	△
2.00	0.65		■		

FIGURE 15. Symbols Used on Type 2 Thermal Crossing Charts.

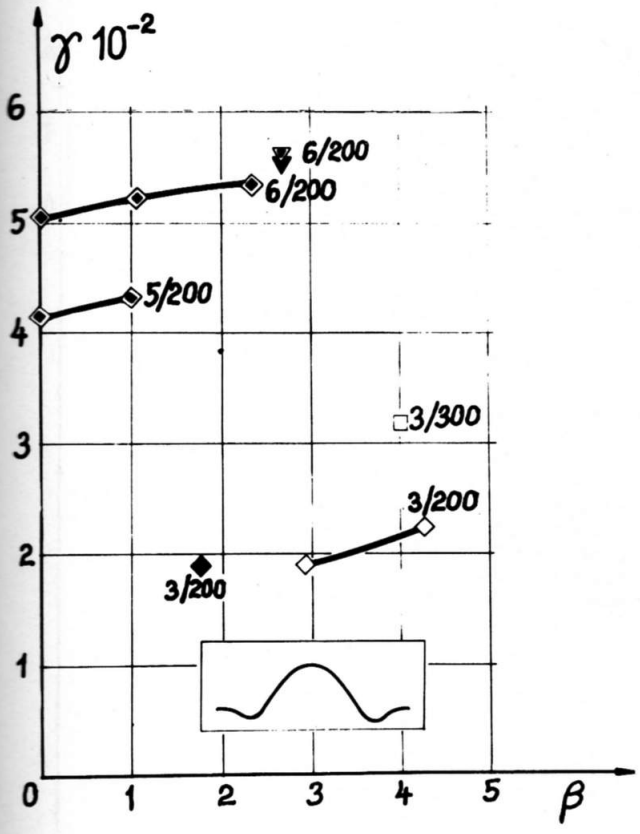

FIGURE 14. Energy Gain Coefficients Calculated for Traverses Through Type 1 Thermals. (Numbers are for c_o/R)

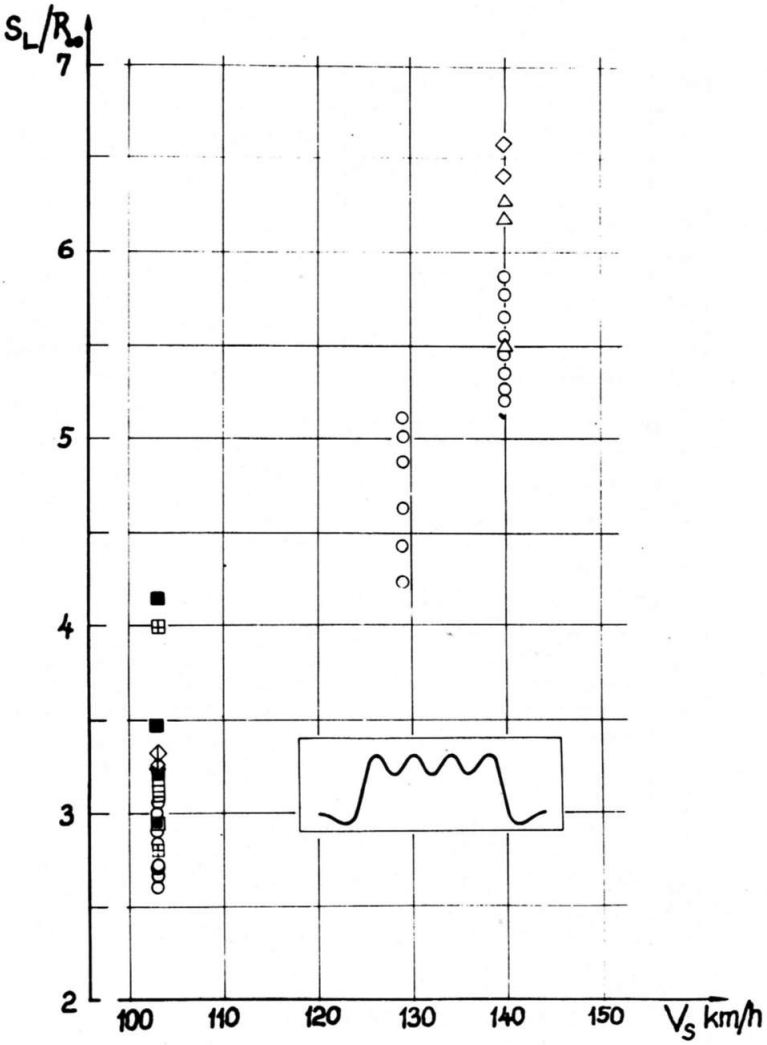

FIGURE 16. Length of Slow-Down in Type 2 2 m/sec Thermal.

TABLE 2. RESULTS OF FOUR-CELL THERMAL TRAVERSE COMPUTATIONS

Run	Flight data						Results									Remarks
	V_s km h^{-1}	V_e km h^{-1}	n_L	n_G	θ_H°	β	$S_L/0.5L$	$S_G/0.5L$	S_L/R_∞	S_G/R_∞	$\gamma\ 10^{-2}$	S/L	V_{AT} km h^{-1}	η_S	η_V	
1	103.296	72.092	1.80	0.70	15	0	0.306	0.384	3.260	4.077	3.950	2.442	90.403	0.772	0.807	
2	"	"	"	"	"	1.0	0.314	0.376	3.330	3.994	4.010	2.482	88.963	0.785	0.800	
3	"	"	"	"	"	2.0	0.306	0.327	3.252	3.475	4.140	2.575	87.686	0.814	0.799	
4	"	"	"	"	18	0	0.390	0.525	3.099	4.173	3.940	2.453	90.205	0.775	0.809	
5	"	"	"	"	"	1.0	0.395	0.502	3.142	3.993	4.021	2.501	88.720	0.790	0.802	
6	"	"	"	"	"	2.0	0.352	0.400	2.800	3.176	4.168	2.538	87.201	0.818	0.803	
7	"	"	"	"	"	3.0	0.502	0.417	3.991	3.313	4.126	2.561	86.669	0.810	0.794	
8	"	"	2.00	0.65	"	0	0.371	0.527	2.948	4.190	3.858	2.402	89.774	0.760	0.797	
9	"	"	1.50	0.70	"	0	0.403	0.601	3.199	4.773	3.962	2.477	90.638	0.782	0.815	
10	"	"	"	"	"	1.0	0.435	0.639	3.461	5.077	4.007	2.518	89.274	0.795	0.810	
11	"	"	"	"	"	2.0	0.406	0.474	3.225	3.769	4.142	2.578	87.708	0.814	0.807	
12	"	"	"	"	"	3.0	0.522	0.500	4.151	3.975	4.115	2.567	86.970	0.811	0.796	
13	139.880	"	1.80	0.56	21	0	0.711	0.994	5.651	7.896	3.826	1.841	107.723	0.702	0.847	
14	"	"	"	"	"	1.0	0.738	1.032	5.863	8.199	3.923	1.907	103.759	0.684	0.829	
15	"	"	"	"	"	2.0	0.654	0.872	5.199	6.932	4.148	1.990	98.974	0.674	0.805	
16	"	"	"	"	"	3.0	0.689	0.731	5.475	5.812	4.422	2.110	97.305	0.703	0.812	
17	"	"	"	"	25	0	0.788	0.818	6.262	6.503	3.754	1.791	108.111	0.690	0.850	
18	"	"	"	"	"	1.0	0.777	1.029	6.172	8.181	3.921	1.906	104.063	0.687	0.834	
19	"	"	"	"	"	2.0	0.689	1.021	5.475	8.113	4.075	1.990	99.110	0.677	0.810	
20	"	"	"	"	"	3.0	0.681	0.887	5.416	7.047	4.398	2.118	96.833	0.709	0.815	
21	"	"	"	"	15	0	0.828	1.096	6.582	8.707	3.584	1.722	110.008	0.686	0.850	
22	"	"	"	"	"	1.0	0.807	1.045	6.413	8.305	3.815	1.832	105.223	0.672	0.832	
23	"	"	"	"	"	2.0	0.790	0.900	6.275	7.156	4.110	1.961	101.850	0.682	0.826	
24	"	"	"	"	"	3.0	0.808	0.861	6.420	6.841	4.355	2.080	99.584	0.710	0.830	
25	129.120	"	"	"	21	0	0.644	0.792	5.116	6.293	3.902	2.022	103.118	0.724	0.850	
26	"	"	"	"	"	1.0	0.532	0.808	4.230	6.420	4.004	2.095	98.164	0.708	0.823	
27	"	"	"	"	"	-2.5	0.582	0.618	4.629	4.909	3.365	1.748	110.905	0.702	0.851	
28	"	"	"	"	"	-1.5	0.556	0.816	4.420	4.897	3.746	1.942	107.326	0.731	0.863	
29	"	"	"	"	"	-0.5	0.632	0.721	5.019	5.730	3.860	2.000	104.784	0.728	0.859	
30	"	"	"	"	"	0.5	0.614	0.854	4.876	6.791	3.942	2.062	100.952	0.711	0.838	
31	139.880	72.092	1.80	0.56	21	-2.0	0.727	0.738	5.775	5.867	3.262	-	-	-	-	$s < 10^2$
32	"	"	"	"	"	-1.35	0.686	0.701	5.453	5.567	3.542	1.691	113.211	0.709	0.860	
33	"	"	"	"	"	-0.7	0.674	0.925	5.356	7.350	3.728	1.782	110.169	0.710	0.857	
34	"	"	"	"	"	-0.05	0.689	1.006	5.474	7.998	3.833	1.850	107.686	0.705	0.850	
35	"	"	"	"	"	3.5	0.695	0.724	5.524	5.754	4.578	2.181	96.585	0.723	0.820	
36	"	"	"	"	"	4.0	0.692	0.731	5.500	5.811	4.726	2.255	95.771	0.740	0.825	
37	"	"	"	"	"	4.5	0.682	0.686	5.420	5.454	4.843	2.311	94.709	0.753	0.825	
38	"	"	"	"	"	5.0	0.663	0.708	5.269	5.627	4.918	2.346	93.301	0.755	0.817	
39	103.296	"	"	"	"	1.5	0.343	0.459	2.723	3.650	4.077	2.540	87.808	0.805	0.801	
40	"	"	"	"	"	2.0	0.327	0.400	2.598	3.179	4.143	2.575	87.055	0.815	0.802	
41	"	"	"	"	"	2.5	0.340	0.372	2.699	2.958	4.155	2.582	86.290	0.819	0.796	
42	"	"	"	"	"	3.0	0.385	0.377	3.062	2.993	4.158	2.583	85.909	0.820	0.792	
43	"	"	"	"	"	3.5	0.392	0.351	3.114	2.791	4.150	2.581	85.192	0.813	0.785	
44	"	"	"	"	"	4.0	0.388	0.355	3.083	2.825	4.129	2.570	84.331	0.814	0.775	
45	"	"	"	"	"	4.5	0.382	0.367	3.034	2.920	4.100	2.550	83.454	0.809	0.763	
46	"	"	"	"	"	5.0	0.376	0.375	2.985	2.979	4.072	2.535	82.595	0.803	0.753	
47	"	"	"	"	"	1.0	0.352	0.494	2.794	3.925	4.003	2.499	88.469	0.794	0.803	
48	"	"	"	"	"	0.5	0.355	0.517	2.825	4.108	3.943	2.463	89.175	0.782	0.805	
49	"	"	"	"	"	0	0.351	0.519	2.792	4.121	3.918	2.445	89.939	0.777	0.806	
50	"	"	"	"	"	-0.5	0.334	0.504	2.657	4.006	3.924	2.446	90.720	0.777	0.815	
51	"	"	"	"	"	-1.0	0.365	0.442	2.899	3.510	3.941	2.451	91.864	0.783	0.824	
52	"	"	"	"	"	-1.5	0.405	0.340	3.217	2.702	3.911	2.433	93.051	0.784	0.833	
53	"	"	"	"	"	-2.0	0.411	0.369	3.268	2.934	3.838	2.386	93.874	0.773	0.831	
54	"	"	"	"	"	-2.5	0.386	0.355	3.068	2.818	3.770	2.343	94.490	0.764	0.828	

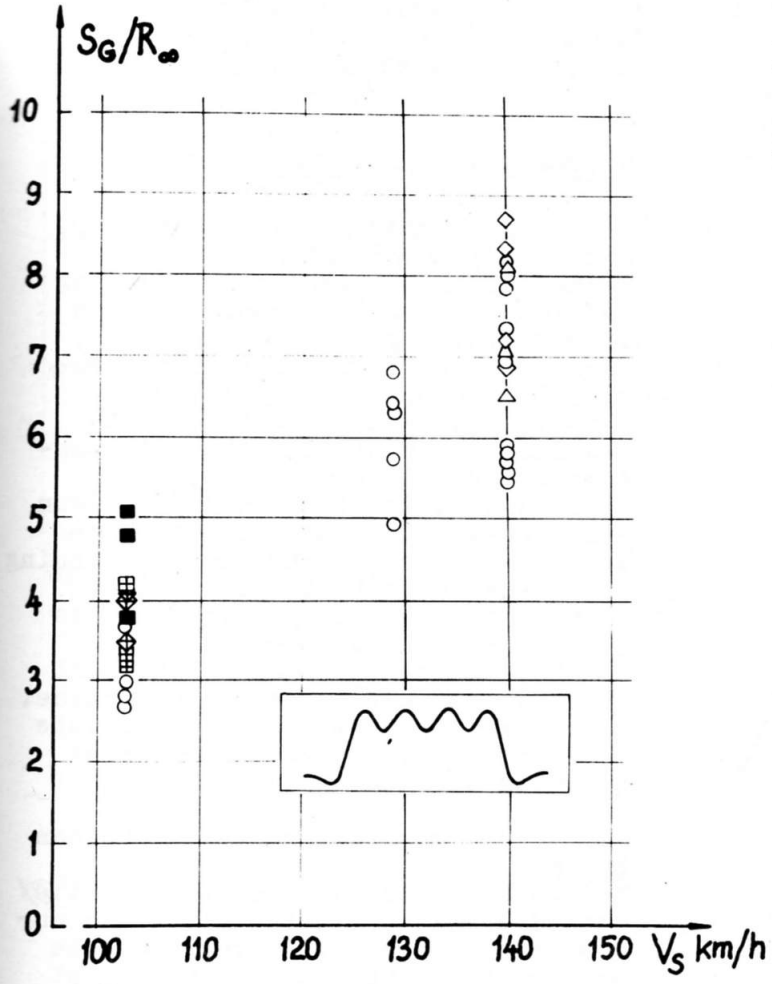

FIGURE 17. Length of Re-Accelerating in Type 2 2 m/sec Thermal.

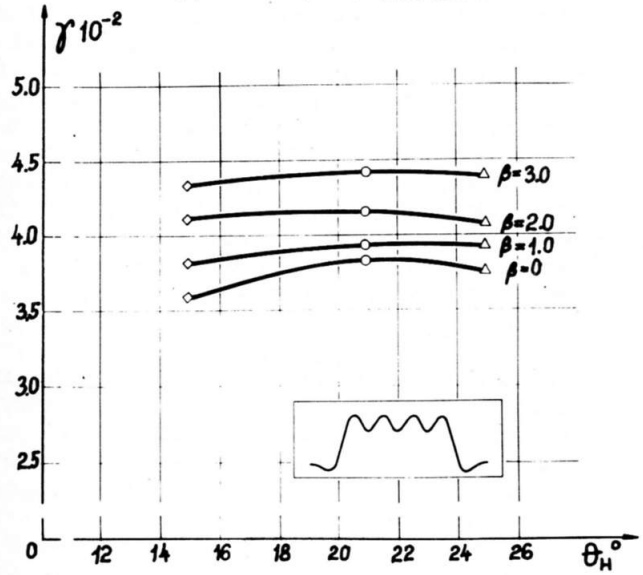

FIGURE 18. Influence of Climb Angle on the Energy Gain in Type 2 2 m/sec Thermal.

The best place to initiate pull-up for the greatest energy gain may be examined on Fig. 19. As concluded from Fig. 13 for single-cell thermals, an early pull-up, before entering the updraft area, is to be recommended. If the glide speed between thermals is V_s = 103 km h^{-1} (i.e. at ϵ_{opt}), then the best value is around $\beta \cong 2.5$ to 3.0 and in this case not much harm is done by disregarding this value. There is even a second, local optimum in the core being, however, without practical significance.

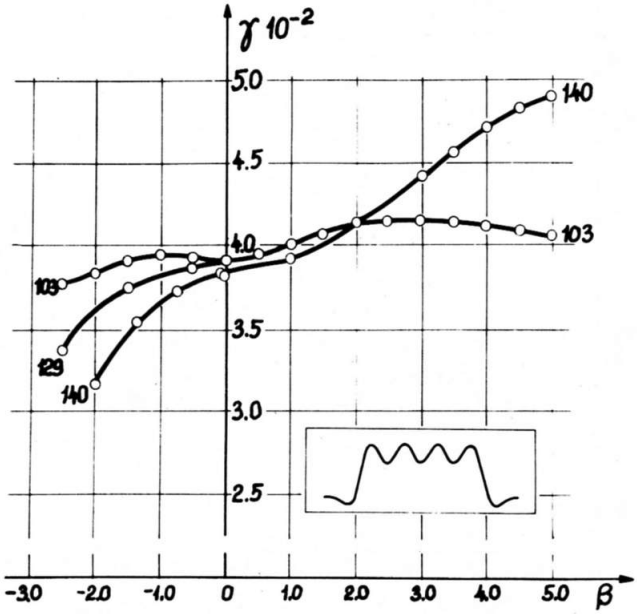

FIGURE 19. Influence of the Pull-Up Point on the Energy Gain in Type 2 2 m/sec Thermals.

For higher glide speeds, the place for optimum pull-up shifts outwards to β = 5.0 and greater values and performance differences are accentuated. It pays, therefore, to have an eye on this but more of it later.

A general view of all results in V_{AT} - S/L co-ordinates is given on Fig. 20. As correctly anticipated on Fig. 12, the best gliding distance obtainable decreases from the idealized $(S^*/L)_{max} \cong 3.16$ to $(S/L)_{max} \cong 2.59$ and for a given value of S/L a fall of 17 to 20 km h^{-1} in cross-country speed V_{AT} as against V^*_{AT} has

been registered. While accepting the general validity of the best load factor and climb angle values obtained for energy gain for all purposes, the influence of the pull-up lead on the glide coefficient and on the speed coefficient may be worth further investigation.

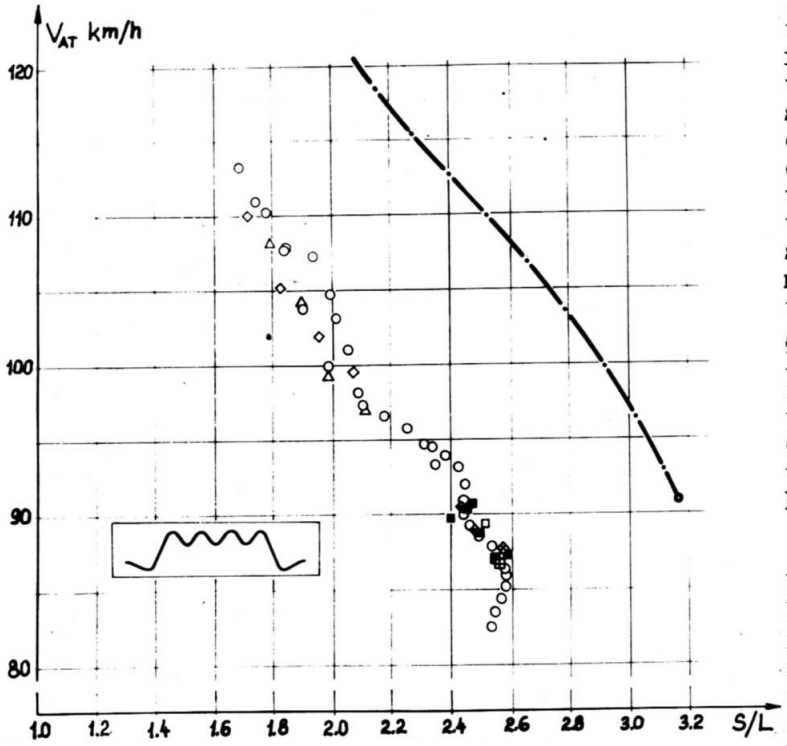

FIGURE 20. General View of Type 2 2 m/sec Thermal Traverse Results.

Fig. 21 shows glide coefficient values as function of the lead coefficient for three different glide speeds V_s. β values for best glide distance are in fairly close agreement with those for optimum energy gain, consequently no need is apparent for modifying maximum energy gain flight technique.

A different story is seen in Fig. 22. Speed coefficient against β curves may show dual optima, but best conditions are to be found here in the thermal core somewhere between $\beta = -1.0$ and $\beta = -1.5$. Allowing for pilot reaction time, for neuromuscular lag and for the lag time of the sailplane longitudinal short period motion, the best moment to initiate the pull-up would be about when entering the thermal lift or a little later, depending on the glide speed.

8. Practical Consequences

When comparing Figs. 19 and 20, a clear speed advantage of the sustained dolphin flight over circling tactics for equal thermal strength is apparent - provided, of course, there is a high enough thermal density L/S to make it possible. In case the thermal strength/density combination is strong enough to sustain higher glide speeds between thermals, flight tactics for optimum speed coefficient are to be recommended. A possible basis for planning the glide could be the net height gain in the thermal we are about to leave. For steady cross-country flight, the height loss to the next thermal must not be above this value. Charts and instruments to facilitate this calculation would be of great help for advanced glider pilots.

Speed coefficient technique can be employed up to the S/L value bridgeable with the best glide ratio/retarded pull-up flying mode. In our numerical example this point may be assumed to be near to run No. 52 at about S/L = 2.433. Still higher values of S/L can be achieved by advancing the pull-up point up to the lead coefficient for best glide at this speed. In our case run, No. 6 is showing the greatest thermal spacing with S/L = 2.588. The gap between the greatest glide distances obtainable using different techniques is, therefore, not significant - in the afore-mentioned case 151 m - being well within the probable error in estimating the distance between thermals.

In the case of a pilot approaching in a high speed glide a thermal he wishes to traverse without circling, and he estimates the glide distance to the next one to be critical for further pure dolphin-style flying, he has to reduce speed immediately. At first he has to change to the optimum glide speed and in the second step, some 100 m before entering the lift, pull-up has to be initiated.

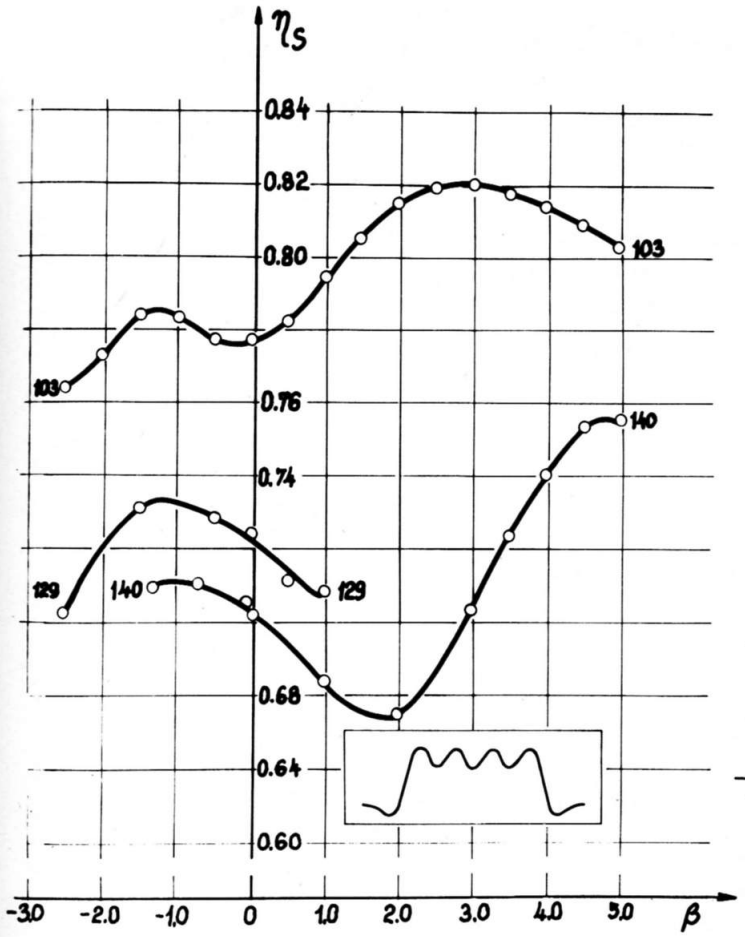

FIGURE 21. Influence of Pull-Up Point on Glide Coefficient. (Numbers are for glide speed between thermals)

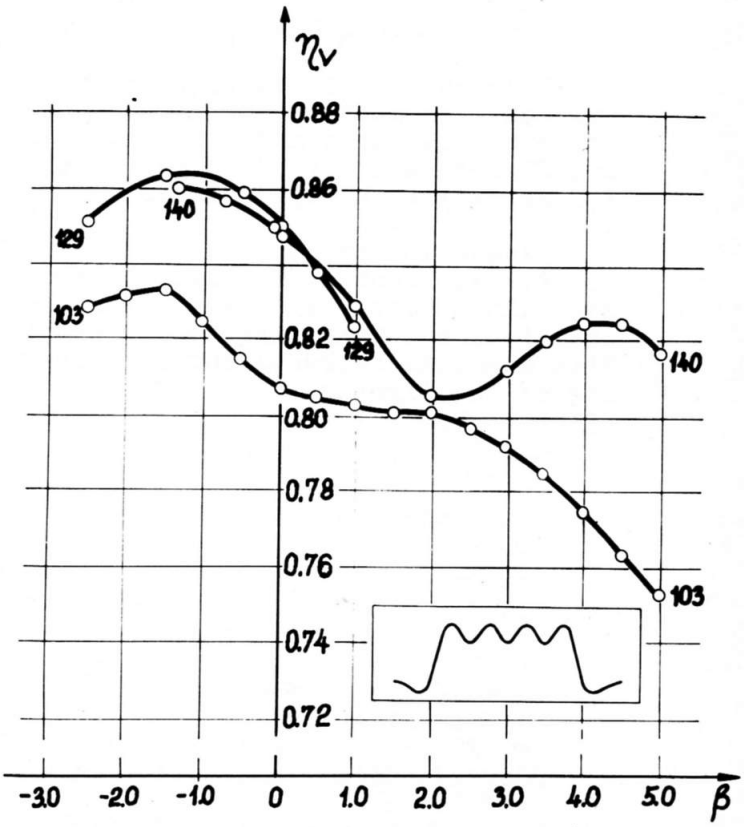

FIGURE 22. Influence of Pull-Up Point on Speed Coefficient. (Numbers are for glide speed between thermals)

For 140 km h^{-1} glide speed, the difference between the glide distance in the best speed and best glide modes amounts to some 370 m, so the technique is well worth the trouble.

Between the greatest S/L for pure dolphin flight and the S/L value corresponding to the H/S value for optimum MacCready glide speed there is usually a fairly wide gap, the domain of mixed flight tactics. Investigations have not been extended to cover this flying mode too so far, but perhaps some of our results may, in a remodelled form, be of some use here too.

SUMMARY

Single and four-cell thermal traverses in dolphin flight have been calculated. Dynamic treatment of the problem was made possible by the use of a finite element method employing three types of path elements. Results have been analysed by calculating the value of the energy gain coefficient and by making comparisons with idealized "square" thermal crossings in glide and speed performances. Results obtained so far seem to recommend the following flight technique:

a. A medium level of load factors and climb/dive angles (e.g.: $n_L = 1.8$, $n_G = 0.56$, $\theta_H = 21^\circ$) should be chosen.

b. For optimum energy gain and for best glide distance, the pull-up should be started some $3R_\infty$ to $5R_\infty$ before entering the up-draft. For best cross-country speed, the best pull-up point is in the thermal core, at a distance $1.0R_\infty$ to $1.5R_\infty$ from the nominal radius.

ACKNOWLEDGMENT

The author wishes to thank Prof. Dr. Pal Michelberger for making possible the research and to Prof. Dr. Elemer Racz for consultation and for his valuable suggestions.

Acknowledgement is due also to Mr. Attila Agoston, Mr. Laszlo Harcz, Miss Ilona Gaspar and Miss Krisztina Huszti of the Computing Center and to Miss Magdolna Petranyi for neat drawing of the figures.

REFERENCES

1. Gedeon, J.: Dynamic Analysis of Dolphin-Style Thermal Cross-Country Flight. Part I, TECHNICAL SOARING, OSTIV Publication XII.

2. Bohli, H. : Optimale Delphinfluggeschwindigkeit auf Streckenflugen. Aero Revue 1971. Nr. 8, August, pp. 391-393.

3. Tomczyk, A.: Przelot bezkrazienia. Skrzydlata Polska, 1972. Nr. 18, 30 Apr.

4. Antweiler, P.: Zur Theorie des Delphinstils. Luftsport, Jahrgang 7. Nr. 6, Juni 1972, pp. 13.

5. Woodward, B.: A Theory of Thermal Soaring. Aero Revue 1958. Nr. 6, June.

6. Konovalov, D. A.: On the Structure of Thermals. OSTIV Publication XI.

7. Milford, J.: Some Thermal Sections Shown by an Instrumented Glider. OSTIV Publication XII.

8. Favanger, D.: Vitesse de croisiere d'un planeur utilisant des rues de nuages. Aero Revue 1968. Nr. 12, December, pp. 645-646, 1969. Nr. 1, January, pp. 27-28.